Ballistic phonon production in photoexcited Ge, GaAs, and Si

M. E. Msall
Department of Physics, Bowdoin College, Brunswick, Maine 04011

J. P. Wolfe
Department of Physics and Frederick Seitz Materials Research Laboratory, University of Illinois at Urbana–Champaign, Urbana, Illinois 61801

(Received 24 October 2001; revised manuscript received 22 January 2002; published 23 April 2002)

Phonon imaging and photoluminescence measurements are used to determine the frequency and spatial distribution of optically generated nonequilibrium phonons in Si, Ge, and GaAs at 1.7 K. At low excitation levels the thermalization of photoexcited carriers and the subsequent phonon down-conversion produce a broad frequency distribution of acoustic phonons that ''quasidiffuse'' in the crystal. These phonons produce a temporally broad heat pulse when detected at a distance from the excitation point. At moderate excitation levels (typically a 10-nS pulse with a power density of $\sim$20 W/mm^2), the laser pulse produces a dense electron-hole plasma that can radically change the frequency distribution of nonequilibrium phonons. The plasma is a potentially rich source of low-frequency acoustic phonons, characterized by a temporally sharp heat pulse at a remote detector. The fraction of low-frequency phonons in the heat pulses is smallest in the direct-gap semiconductor GaAs, where rapid recombination depletes the populations of electrons and holes in just a few nanoseconds. More noticeable low frequency phonon components are seen in heat pulses in the indirect-gap semiconductors Ge and Si. At sufficiently high excitation densities ($\sim$60 W/mm^2) in Ge, there is a suppression of the low-frequency phonon signal, which may result from phonon absorption within a cloud of electron hole droplets. An interesting alternative hypothesis is that the acoustic phonons created in the plasma are sufficiently dense to initiate phonon coalescence, whereby phonons are localized by phonon-phonon scattering over a relatively long period (500 ns). This localized ''hot spot'' could provide the phonon wind that drives the initial rapid expansion of the electron-hole plasma into the crystal.

DOI: 10.1103/PhysRevB.65.195205 PACS number(s): 71.35.Ee, 63.20.Kr

I. INTRODUCTION

Direct photoexcitation of semiconductors at low temperatures produces energetic electrons and holes that thermalize by emission of phonons. The carriers recombine, leaving an expanding cloud of nonequilibrium phonons. By detecting the time evolutions of (a) the recombination luminescence of the excited carriers, and (b) the thermal energy arriving at a remote point, one can indirectly study the transfer of energy mediated by electron-phonon and phonon-phonon processes. We have conducted a series of such experiments on Si, Ge, and GaAs, and found that the frequencies and spatial distributions of phonons produced through optical excitation depend radically on the optical excitation level.

Different regimes of phonon production in photoexcited semiconductors can be accessed by changing the ''excitation density,'' or absorbed laser power per area. At *low excitation densities* each photoexcited carrier thermalizes without extensive carrier-carrier interactions. Single-carrier relaxation produces a broad band of phonons that propagate and down-convert in a process known as quasidiffusion.[1] Quasidiffusion is observed in Si, Ge, and GaAs at low levels of photoexcitation.[2] At moderate to high levels of photoexcitation the build-up of phonon and carrier populations affects the frequency and spatial distribution of the phonons. Earlier work on photoexcited Si showed that, even at moderate excitation levels, carrier-carrier interactions effectively reduce the broad frequency distribution associated with quasidiffusion.[3]

In the present work, we attempt to generalize our understanding of the interplay between nonequilibrium phonons and photoexcited carriers to two other semiconductors with very different electronic properties, namely, Ge and GaAs. The electronic band structures and carrier lifetimes are particularly relevant to the phonon dynamics at high carrier densities. GaAs is a direct-gap semiconductor with an exciton lifetime of only about 0.5 ns, and a similarly short-lived electron-hole plasma. In contrast, Ge is an indirect-gap semiconductor (like Si) in which stable electron-hole liquid (EHL) is formed by photoexcitation at low temperatures. The density of the EHL in Ge, however, is an order of magnitude lower than that in Si, causing a lifetime 300 times longer. Thus, these two materials (GaAs and Ge) provide informative contrasts to the earlier studies of nonequilibrium phonon production in Si.

II. EXPERIMENTAL DETAILS

The experiments reported in this paper use heat-pulse and phonon-imaging techniques.[4] The samples are as follows: (1) A $2.6\times3\times1.35$-mm^3 GaAs sample, meltgrown by Wacker Chemitronics in a BN crucible. We thank W.E. Bron of the University of California at Irvine for this sample. It is ''chromium free'' with a resistivity of $\rho=10^6\ \Omega$ cm. (2) An $8\times9.1\times3$-mm^3 ultrapure dislocation-free Ge crystal (Boule 146) grown by E.E. Haller at Lawrence Berkeley Laboratory. (3) Two undoped Si samples grown by Siemens, one with dimensions $6.6\times7.0\times5.4$ mm^3, and the other 8.9×8.7

$\times 2.75\ \mathrm{mm}^3$. Both are characterized by $N_A - N_D = 10^{12}\ \mathrm{cm}^{-3}$.

For all crystals, the excitation and detection faces are {100} planes. The samples were mechanically polished with an alumina suspension and polished and etched with Syton to remove subsurface damage. The detectors are $10 \times 5\text{-}\mu\mathrm{m}^2$ granular-aluminum bolometers directly evaporated on the largest faces. The superconducting transitions of the bolometers were just below 2 K. These detectors are current biased, and characterized by their response to direct photoexcitation with a 10-ns laser pulse. This excitation typically produces a voltage pulse with a full-width at half-maximum of 70 ns, indicating the time resolution of the experiment.

All experiments are performed with direct photoexcitation of the crystal surface by a focused laser pulse (in contrast to exciting a metal film on the crystal surface). We typically use a cavity-dumped Ar^+ laser with a 10-ns pulse width. The laser is focused to a spot with full-width at half-maximum (FWHM) of approximately 10 μm, and we define the power density as peak absorbed power divided by the laser spot area ($\pi \mathrm{FWHM}^2/4$) in units of $\mathrm{W/mm}^2$. The detector surface and the four sidewalls are always in contact with the liquid He at 1.7 K, but the excitation surface has a vacuum interface, isolated from the He bath by the sample holder as in Ref. 2. This configuration eliminates the complexities of a fluid contacting the excitation surface (e.g., phonon loss into the He bath, He bubbles, etc.).

The green laser light produces energetic electrons and holes within one optical absorption length of the excitation surface, which is less than 1 μm. In order to monitor the electrons and holes, we measure the photoluminescence in Si and Ge under the same excitation conditions as the phonon experiments. Since the crystals are transparent to luminescence from carrier recombination, the luminescence can be conveniently collected from the detection surface of the sample: the area of the detection surface covered by the bolometer films and contact pads is a small fraction of the available surface area. The recombination luminescence is imaged onto the entrance slit of a $\frac{1}{4}$-m $f/3.5$ spectrometer. A Ge *p-i-n* diode operated in the photoconductive mode is located at the exit slit of the spectrometer, and the induced photocurrent is amplified by a low-noise current preamplifier.[5] Because the radiative efficiency is weak in Si (about 0.1%), the signals resulting from even our highest power laser pulse are rather small. To improve the signal level in this case we modulate the pulse train at low frequency and use lock-in signal detection, making temporally resolved measurements impossible. In Ge, where the optical quantum efficiency is larger, boxcar detection is possible, and we are able to spatially and temporally resolve the luminescence signal following pulsed excitation.

III. BALLISTIC PHONONS

Green excitation ($h\nu = 2.4$ eV) produces free carriers with large kinetic energies because the semiconductor energy gaps are in the infrared. Thus the initial source of nonequilibrium phonons is hot-carrier thermalization. These phonons inelastically down-convert to lower frequencies, and elastically scatter from mass defects as they travel from the excitation point to the detector. The shape of the detected pulse depends upon the propagation direction between source and detector and the rate of phonon scattering and absorption in the crystal. Phonons with mean free paths comparable to the sample dimensions are said to travel ballistically (i.e., without scattering) through the sample. The ballistic phonon flux has a strong dependence on the propagation direction due to phonon focusing, which is a natural consequence of the crystalline anisotropy.[4] This anisotropy is typically mapped by a phonon image which shows the flux intensity as a function of laser position on the excitation surface.

Phonon images taken at moderate excitation powers with a well-focused laser show sharp and strong changes in the detected flux as a function of laser position relative to the detector as predicted by the continuum acoustic model. This implies that the ballistic phonons are predominantly low frequency ($\nu \leqslant 500$ GHz). The sharpness of the singularities in phonon flux (caustics) indicate that the low-frequency phonons originate from a source region with dimensions comparable to the area illuminated by the laser. Phonons that scatter from defects or impurities enroute to the detector cause a broad background in the phonon image.[6]

Ballistic phonons can also be identified by their short propagation times in the sample. The ballistic time is defined to be the minimum time required for a phonon to cross the sample. When the propagation direction is near to, but not directly along, a caustic direction, the phonon pulse is dominated by diffusive phonons. Since the diffusive pulse component is not highly anisotropic, the subtraction of two phonon pulses, one on a sharp caustic and the other slightly displaced from the caustic position, isolates the ballistic component.[7] Comparison of the integrated signal at on- and off-caustic positions show that ballistic phonons comprise only a small part of the signal along the caustic direction (typically 10–20 % of the total energy). The fraction of ballistic phonons arriving along a noncaustic direction is even smaller. It is the concentration along certain crystalline directions by the phonon focusing effect that makes the ballistic flux so noticeable.

A Monte Carlo computer simulation of ballistic phonon propagation from a point source, including phonon focusing effects and a detector size equal to our experimental detector size, can provide a measure of the expected phonon-focusing enhancement along particular crystalline directions. The directionally dependent phonon focusing enhancement factor[8] can then be used to determine the overall ratio of ballistic to scattered phonons by making measurements along a few crystalline directions. Under focused excitation (in the high excitation density, nonquasidiffusive regime) this proportion is highest in Ge, where an estimated 4–9 % of the phonons reaching the opposite side of the crystal are ballistic over the range of deposited energy available in our experiments. In Si, 3–5 % of the detected signal is ballistic at the same excitation levels, while in GaAs, the ballistic signal is only 1–2 %. In all crystals studied, however, the proportion of ballistic signal detected is significantly affected by excitation conditions.

IV. ENHANCED BALLISTIC FLUX AT HIGH EXCITATION DENSITIES

In the low excitation density regime ($\leqslant$10 W/mm^2), most of the excess energy ($h\nu_{\text{photon}} - E_{\text{gap}}$) imparted to the carriers by the laser photons is shed by emitting optical phonons. These optical phonons do not travel far in the crystal before decaying into acoustic phonons. As the acoustic phonons diffuse into the bulk of the crystal, they continue to undergo anharmonic decay to lower frequencies. The combination of diffusion and anharmonic decay scattering results in ''quasidiffusive'' heat pulses characterized by long diffusive tails.

The key requirements[2] for observing quasidiffusive phonon pulses are (a) the excitation surface must be isolated from the liquid helium bath, and (b) the density of excited carriers produced by the laser pulse must be sufficiently low. Experimentally, the latter condition is met by illuminating a large area with the laser.

If the density of photoexcited carriers is increased by decreasing the size of the laser focal spot on the crystal without changing the pulse energy, the phonon signal near the ballistic time, t_b, is greatly increased. This increase in ballistic phonons at high excitation density is most clearly seen by plotting the peak intensity of the detected heat pulse scaled by the absorbed power (Fig. 1). The absorbed power (indicated in the legend) is the average laser power during the 10-ns pulse for a given data set; the power density is varied by changing the size of the focal spot.

The proportion of the deposited energy that produces ballistic phonons is independent of the total power deposited (at a given power density) in Si [Fig. 1(a)] and GaAs [Fig. 1(b)], with a clear transition in the character of the heat pulse above a power density of 20 W/mm^2. The data for Ge do not follow this trend. As shown in Fig. 1(c), the ballistic phonon signal in Ge does increase with increasing power density, but the amount of increase appears to depend on the total energy in the phonon pulse. Furthermore, the flux at the ballistic time unexpectedly decreases at the highest excitation levels. These interesting effects will be discussed in detail in Sec. VI. For now, we focus our attention on the increase in the proportion of ballistic phonons seen in all three materials at excitation densities near 20 W/mm^2.

The magnitude of the increase in the ballistic phonons as the excitation density is raised is typically a factor of 3–5 in our experiments. This increase is attributed to the effect of carrier thermalization in the presence of large numbers of other carriers. Essentially, at high excitation density some of the newly excited carriers within the excitation pulse bypass the optical-phonon emission channel in favor of cooling by intercarrier scattering, with the partially thermalized carriers created in an earlier portion of the pulse. The plasma then emits lower-frequency acoustic phonons. This idea was originally developed for Si, where Auger recombination produces a small number of hot carriers within an otherwise cool liquid.[9] Now we find that Ge and GaAs, where Auger recombination plays a lesser role due to lower carrier densities, also show enhanced low-frequency phonon production. Does the bypass theory, developed for Si, apply in these cases? If so, it seems that the bypass of high-frequency phonon production must occur for the *optically* created hot carriers. Let us consider the case for GaAs.

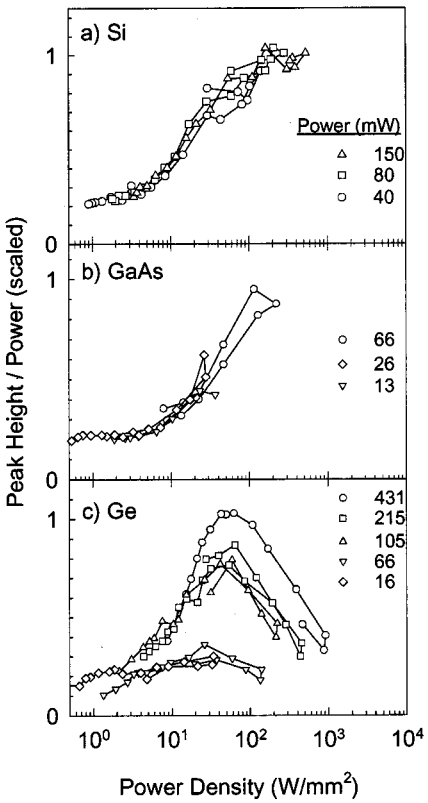

FIG. 1. Phonon intensity near the ballistic time (integrated over $1.0t_b \leqslant t \leqslant 1.2t_b$) as a function of power density, for several different total input powers in: (a) Si, (b) GaAs, and (c) Ge. It should be emphasized that the total energy deposited in the crystal is unchanged for each data set while the size of the excitation region is varied. This technique allows us to achieve high signal levels at low power densities. It is, however, necessary to choose a propagation direction for which the phonon focusing enhancement factor does not vary widely as the focus is changed, so that the data at different focal sizes are easily comparable.

V. HIGH EXCITATION DENSITY IN GaAs

Figure 2 shows time traces for several different incident powers (fixed laser focus) in GaAs. At all powers the exponential decay characteristic of quasidiffusion is present at late times, but at high power there is also a noticeable ''peak'' of phonons arriving near the ballistic time. The amount of energy in this ballistic peak relative to the tail increases as the total energy deposited by the laser is increased. This increase is not due to any change in the focusing of phonons near the excitation point, because the laser focal spot is fixed. The increase signifies an increase in the fraction of locally produced low-frequency phonons.

For GaAs, where the carrier recombination time is less than 1 ns, the 10-ns laser pulse corresponds to a steady-state excitation. Also, after about 1 ns, the temperature of the carriers should reach a steady value above the lattice tempera-

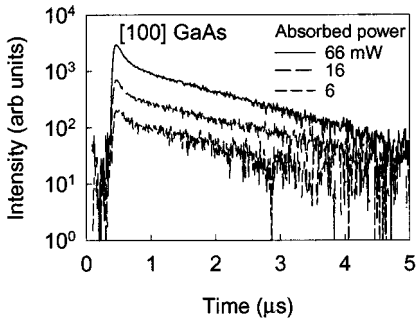

FIG. 2. Experimental time traces along the [100] direction in 1.35-mm-thick GaAs, for several deposited powers. The laser focal spot is the same for all three traces ($d=10\ \mu$m). At high powers there is a noticeable increase in the ''concentration'' of phonons arriving near the ballistic time.

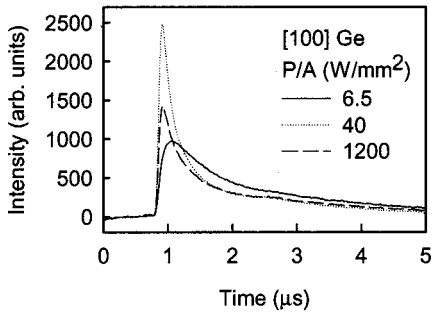

FIG. 3. Experimental timetraces along the [100] direction in 3-mm-thick Ge. In all-traces the input power is constant (about 100 mW during the 10-ns laser pulse) and the excitation density is varied by defocusing the laser. At low excitation density (the solid line) the phonon propagation is quasidiffusive and the energy arriving at the detector is widely spread in time. At intermediate excitation density (dotted line) there is a much greater portion of the signal arriving near the ballistic time, indicating that low-frequency phonons are being produced more rapidly than the quasidiffusive phonon cascade. At high excitation density (dashed line) the signal near the ballistic time is less intense than at intermediate excitation density.

ture due to rapid phonon emission; the experimental basis for this fact is that the carrier temperature, as measured by phonon-assisted photoluminescence, is less than 15 K. At this temperature, the average carrier energy is much less than that of the newly excited carriers. Thus it is plausible that new carriers produced during the pulse cool by carrier-carrier scattering in conjunction with acoustic phonon emission, thereby bypassing the optical-phonon emission channel. The observed ballistic peak at high excitation density is then primarily due to acoustic phonons that are directly emitted from the electron-hole plasma. Relatively few ballistic phonons are produced in GaAs because the band-gap energy is lost by radiative decay in this direct-gap crystal. In contrast, for Si the band-gap energy is a large contributor to the bath of nonequilibrium phonons due to nonradiative recombination. In that case, Auger recombination converts the band-gap energy of an electron-hole pair into kinetic energy of a third particle within the well-thermalized EHL.

VI. HIGH EXCITATION DENSITY IN Ge

Our measurements of phonon pulses in Ge display an onset of ballistic phonon production similar to that in Si and GaAs. However, Ge shows a startling behavior at the highest excitation levels. Instead of a monotonic increase (or leveling off) of the ballistic phonon flux as the power density is raised, there is a pronounced decrease at the highest excitation levels. As the excitation density increases beyond ~40 W/mm^2 the flux arriving at the ballistic time begins to *decrease* and the pulse *broadens* in time, as shown in Fig. 3. Nothing comparable was observed for Si or GaAs, suggesting that Ge has entered a new regime for phonon interactions or production.

At first glance the ballistic phonon production in Ge does not appear to depend on power density alone. For low input powers [Fig. 1(c)] the peak intensities show less variation with excitation density than for high input powers. However, the shape of the near-ballistic phonon pulses in Ge changes dramatically during defocusing (Fig. 3). Thus the narrow time window used to measure the peak signal in the data of Fig. 1 may not capture all of the rapidly produced low frequency phonons in Ge. In Fig. 4 we plot the temporal FWHM of the timetrace. The variation in the FWHM as a function of excitation density does seem to follow a ''universal curve'' relatively independent of the input powers. The pulse width ranges from 200 ns at intermediate excitation density to 1.2 ms at the lowest measured excitation densities.

It appears that in Ge three, rather than two, regimes are observed: quasidiffusion at the lowest excitation; a shift to more ballistic phonon production at intermediate excitation; and a depletion of ballistic phonons at the highest excitation densities. We now consider the special electronic properties of Ge that may lead to these unusual results.

VII. PHONONS AND THE ELECTRON-HOLE LIQUID IN Ge

In Ge, at a temperature below 6 K, metallic droplets of electron-hole liquid form.[10] This EHL has a characteristic

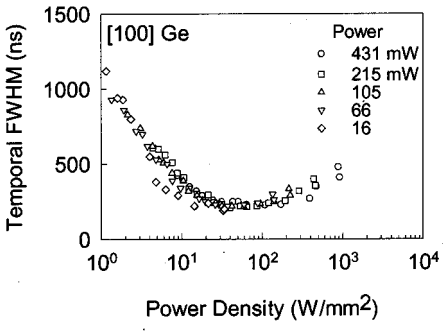

FIG. 4. Full width at half-maximum of the phonon timetraces in Ge as a function of power density. The mean phonon arrival time is smallest at about 50 W/mm^2.

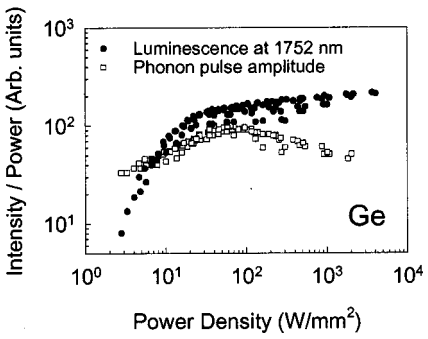

FIG. 5. Detected photoluminescence intensity for Ge at the droplet wavelength ($\lambda = 1.75\ \mu$m) as a function of power density and the phonon peak height for the same excitation conditions. The excitation density is varied by defocusing the laser at five different input powers (cf. Fig. 7). Each set of data is scaled by the input power. The luminescence is collected with a wide input slit on the spectrometer, which effectively integrates the luminescence from a large area on the sample.

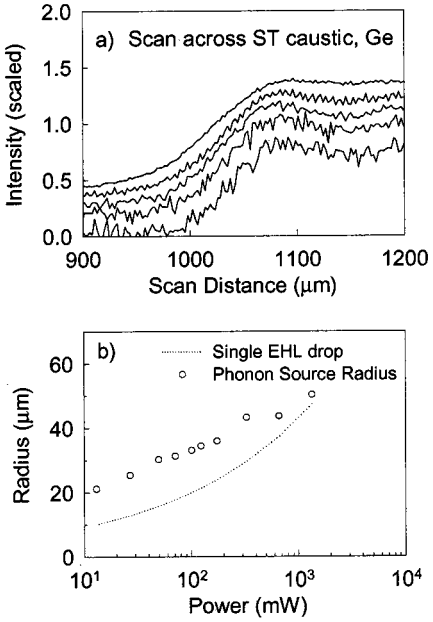

FIG. 6. Measurement of the phonon source radius. (a) The sharpness of the ST box caustic for several different total powers. In descending order, $P = 1.3$ W, 660 mW, 330 mW, 170 mW, and 123 mW. The time window for data collection is within 50 ns of the ballistic arrival time. The phonon source radius is determined by the 10–90 rise in the ballistic phonon signal as the laser is scanned over the caustic. (b) Phonon source radius as a function of power. For comparison, the dotted line shows the calculated radius of a single drop of EHL at the end of a 10-ns pulse as a function of input power. The laser focal radius is constant (9 μm).

luminescence peak at $\lambda = 1.75\ \mu$m, due to electron and hole recombination within a liquid droplet. At the lowest excitation power densities the luminescence signal from the EHL, shown in Fig. 5, is small, but as the power density increases it rises, indicating an increased fraction of the excited carriers condensing into liquid. At the highest excitation densities the luminescence signal saturates, signifying that nearly all of the carriers are in the liquid state. The rise in luminescence from the liquid (between 0.3 and 3.0 W/mm^2) is correlated with the increase in the phonon signal arriving near the ballistic time. This correlation is qualitatively similar to that previously observed in Si. However, in Ge, there is a drop-off in peak height at the highest excitation densities (100–3000 W/mm^2) that is not accompanied by a similar change in the luminescence signal, as in Si. At the highest excitation densities in Ge, the EHL is clearly present, but the portion of detected ballistic phonons is reduced.

A possible mechanism for the reduced ballistic-phonon signal is increased phonon-carrier scattering in a large volume of liquid. Under steady-state excitation, carriers condense into liquid droplets of 1–5 μm radius that are distributed in a millimeter-sized cloud with a filling factor of approximately 1%.[11] For intense pulsed excitation, however, it is possible that a single large drop of EHL is produced during the 10-ns laser pulse. This large drop of liquid will both emit and absorb acoustic phonons.

In Fig. 6 we estimate the ''initial drop'' radius (following the 10-ns pulse) from the number of incident photons and the known EHL density, and compare it to the measured radius of the phonon source. The phonon source size is determined from the sharpness of the caustic formed by slow transverse phonons observed under the best focus conditions, i.e., the sharpness of the ledge in Fig. 6(a). Figure 6(b) shows that the size of the source region is comparable to the area illuminated by the laser at the lowest powers, but grows significantly with increasing power. The phonon source region is somewhat larger than the region that would be occupied by a single EHL drop at all but the highest excitation levels.

As time progresses the initial drop of liquid will disperse into a cloud of droplets. We can measure the ultimate cloud size (before recombination in 40 μs) by imaging the time-integrated luminescence spot radius (Fig. 7). At low powers the radius is about 270 μm, and becomes about 350 μm at the highest powers. These values are from 14 to 7 times greater than the radius of a single drop containing all the carriers, yielding a volume fraction occupied by electron hole liquid of 0.04% to 0.30%. Such a diffuse cloud of droplets would not be effective at trapping phonon energy, but droplets do absorb and re-emit phonons. In fact, absorption by a ''phonon wind'' causes expansion of the exciton cloud.[11]

To account for the small phonon source size, the phonons must be emitted by the EHL early in the liquid expansion. A previous measurement in Ref. 12 of the expansion of EHL in Ge showed that after an initial ''jump-out'' at the EHL density, droplets of liquid are pushed into the crystal by a wind of low-frequency acoustic phonons. Our measurements are shown in Fig. 8. The luminescence spot radius is about 150 μm at 100 ns (the limit of our temporal resolution). After 500-ns it has expanded to the final size of 300 μm. This is roughly three times the size of the measured phonon spot size at a comparable excitation level. The expansion rate

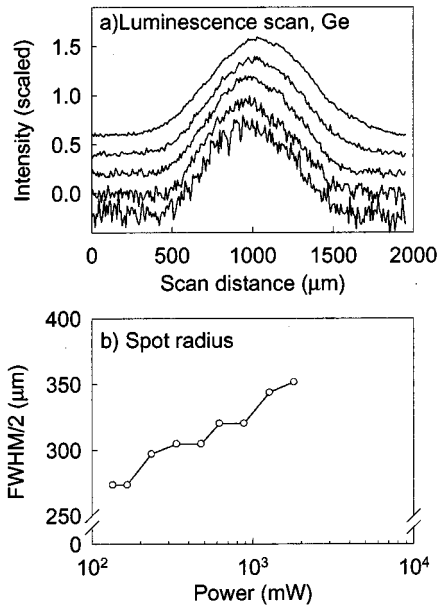

FIG. 7. (a) Spatial scan of the luminescence intensity for five different total powers: In descending order, $P=1.8$ W, 900 mW, 440 mW, 220 mW, and 135 mW. For this time-integrated measurement, lock-in detection is used. The spatial resolution is about 50 μm. (b) The luminescence spot radius is the half-width at half-maximum of the luminescence scans in part a.

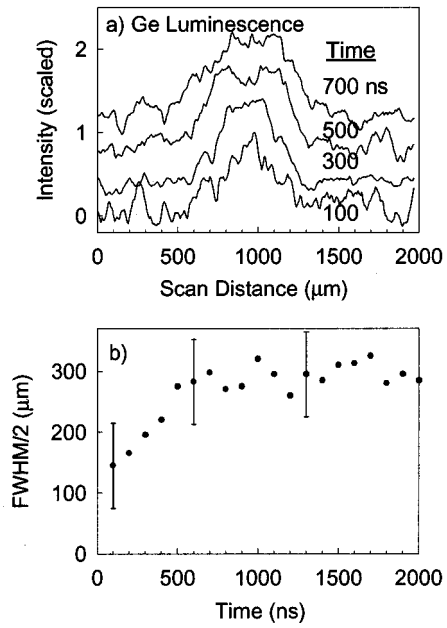

FIG. 8. Time resolved measurement of the spatial extent of the EHL after high power (1.47 W, focused excitation, 80-μs pulse repetition time) excitation. In order to increase the collected signal, a 500-μm input slit is used on the spectrometer yielding a spatial resolution of less than 100 μm. The time resolution of the amplifiers is about 200 ns, and the data collection window is 100 ns long.

corresponds to a linear velocity of 0.3×10^5 cm/s, roughly one-tenth of the velocity of sound. The sudden halt in the expansion after 500 ns appears to mark the end of net outward pressure on the droplets (i.e., the phonon wind). This expansion time is of the same order as the width of the ballistic phonon pulse shown in Fig. 3 (also 500 ns at high excitation). Thus a possible explanation for the reduced ballistic flux at high excitation densities is simply that the cloud of droplets causes an additional scattering of the otherwise ballistic phonon flux. An effective attenuation of the ballistic signal requires a spatially concentrated electron-hole liquid, however, and our measurements of the cloud size suggest that we are creating a diffuse cloud.

Another effect that may play an important role in the temporal behavior of the phonons is the build-up of high phonon occupation numbers at early times, which could lead to the localization of energy by phonon-phonon scattering processes; i.e., a phonon ''hot spot.'' [13] The hot spot could be the source of the phonon wind that drives the initial rapid expansion of the electron-hole plasma in the crystal. In the case of a pure phonon hot spot without phonon-carrier interactions, the hot spot is only a source of ballistic phonons for as long as the typical phonon mean free path is less than the effective spot size. As the spot spreads and cools, it no longer effectively confines low-frequency phonons and becomes a quasidiffusive ''decay spot.'' The lifetime of the pure hot spot is predicted[14] to depend linearly on the deposited energy E, while its size varies as $E^{0.47}$. In our Ge experiments the observed phonon source size increases $\sim E^{0.18}$, which suggests that a more detailed model that includes both phonon-carrier and phonon-phonon interactions is necessary.

VIII. CONCLUSIONS

Beyond the quasidiffusive regime the production of phonons in photoexcited semiconductors is strongly influenced by the excitation density (the absorbed laser power per area). At moderate excitation densities the population of quasidiffusive phonons is reduced in favor of rapid production of low-frequency phonons, as carriers bypass the optical-phonon emission channel in favor of cooling by intercarrier scattering and acoustic-phonon emission within the electron-hole plasma. This effect occurs at about the same excitation power densities for Si, GaAs, and Ge. Because the recombination rates are vastly different in these three semiconductors, the similar behavior of ballistic phonons suggests that the key processes occur during the short excitation pulse.

For Si, significant production of high-energy carriers continues well after the 10-ns excitation pulse because Auger heating results in continual production of acoustic phonons by the electron-hole liquid. In GaAs, the much shorter recombination time precludes carrier interactions after the laser pulse, so that the production of acoustic phonons by carriers is very brief. In Ge, the weak Auger recombination processes in the EHL produce a weak acoustic phonon emission, implying that the principal source of high frequency phonons occurs during the initial thermalization process. Thus, at low to medium excitation levels, the production of acoustic

phonons by the carriers is brief. However, at the highest excitation levels in Ge the arrival of acoustic phonons is spread over a longer time. A full understanding of the factors that suppress the ballistic phonon signal at the highest excitation density requires a detailed model that predicts the frequency and spatial distributions of the phonons and carriers and their interactions. Our heat pulse data offers some motivation to examine these processes and possibly a new testing ground for such models.

ACKNOWLEDGMENTS

We thank S. Espov for his stimulating input to this project. The work was supported in part by the National Science Foundation (Materials Research Laboratory Grant No. DEFG02-91ER45439), the GAANN Fellowship program, and the AFOSR under Contract No. F49620-00-1-0328 through the MURI program.

[1] D. V. Kazakovtsev and Y. B. Levinson, Phys. Status Solidi B **96**, 117 (1979); W. E. Bron, Y. B. Levinson, and J. M. O'Connor, Phys. Rev. Lett. **49**, 209 (1982).
[2] M. E. Msall and J. P. Wolfe, Phys. Rev. B **56**, 9557 (1997).
[3] M. E. Msall, S. Tamura, S. E. Esipov and J. P. Wolfe, Phys. Rev. Lett. **70**, 3463 (1993).
[4] James P. Wolfe, *Imaging Phonons, Acoustic Wave Propagation in Solids* (Cambridge University Press, Cambridge, 1998).
[5] A comparable setup is shown in M. Greenstein and J. P. Wolfe, Phys. Rev. B **26**, 5604 (1982).
[6] M. T. Ramsbey, J. P. Wolfe, and S. Tamura, Z. Phys. B: Condens. Matter **73**, 167 (1988).
[7] M. Greenstein and J. P. Wolfe, Phys. Rev. B **24**, 3318 (1981).
[8] H. J. Maris, J. Acoust. Soc. Am. **50**, 812 (1971).
[9] S. E. Esipov, M. E. Msall, and J. P. Wolfe, Phys. Rev. B **47**, 13 330 (1993).
[10] P. Vashishta, S. G. Das, and K. S. Singwi, Phys. Rev. Lett. **33**, 911 (1974); J. C. Hensel, T. G. Phillips, T. M. Rice, and G. A. Thomas, *Solid State Physics*, edited by H. Ehrenreich, F. Seitz, and D. Turnbull (Academic, New York, 1977), Vol. 32.
[11] *Electron-hole Droplets in Semiconductors*, edited by C. D. Jeffries and L. V. Keldysh (North-Holland, Amsterdam, 1983).
[12] M. Greenstein, M. A. Tamor, and J. P. Wolfe, Solid State Commun. **45**, 355 (1983).
[13] D. V. Kazakovtsev and Y. B. Levinson, Zh. Eksp. Teor. Fiz. **88**, 228, (1985) [Sov. Phys. JETP **61**, 1318 (1985).]
[14] Y. B. Levinson, in *Laser Optics of Condensed Matter*, edited by E. Garmire, A. A. Maradudin, and K. K. Rebane (Plenum, New York, 1991), Vol. 2, pp. 361–367.